Table S1. List of the siRNA sequences

Name	Primer sequence
Si-IRF-1 sense	5'-CAGAUAUCGAGGAGGUGAATT-3'
Si-IRF-1 antisense	5'-UUCACCUCCUCGAUAUC UGTT-3'
Negative control sense	5'-UUCUCCGAACGUGUCACGUTT-3'
Negative control antisense	5'-ACGUGACACGUUCGGAGAATT-3'

Table S2. List of the primer sequences

Primer name	Primer sequence
H-IRF-1 F	GCATGGCTGGGACATCAAC
H-IRF-1 R	TTCCTGCTCTGGTCTTTCACCT
H-RAD51 F	ACTGCTCCCTGGGGTTCTC
H-RAD51 R	TTCCTAAGGCACCATGTCAAAG
H-GAPDH F	AATCCCATCACCATCTTCCAG
H-GAPDH R	GAGCCCCAGCCTTCTCCAT

Table S3. List of the sequences of the primers surrounding the putative binding sites for IRF-1 from RAD51 gene promoter region

Primer name	Primer sequence
Site-1-F	AGTACCTAGAGACCAAAGCTCCT
Site-1-R	GAAGTGCTTGAACCCGGGAG
Site-2-F	TGAGACCACAGGCACAAGCC
Site-2-R	ATATAAGGCCTGCACGGTGGC

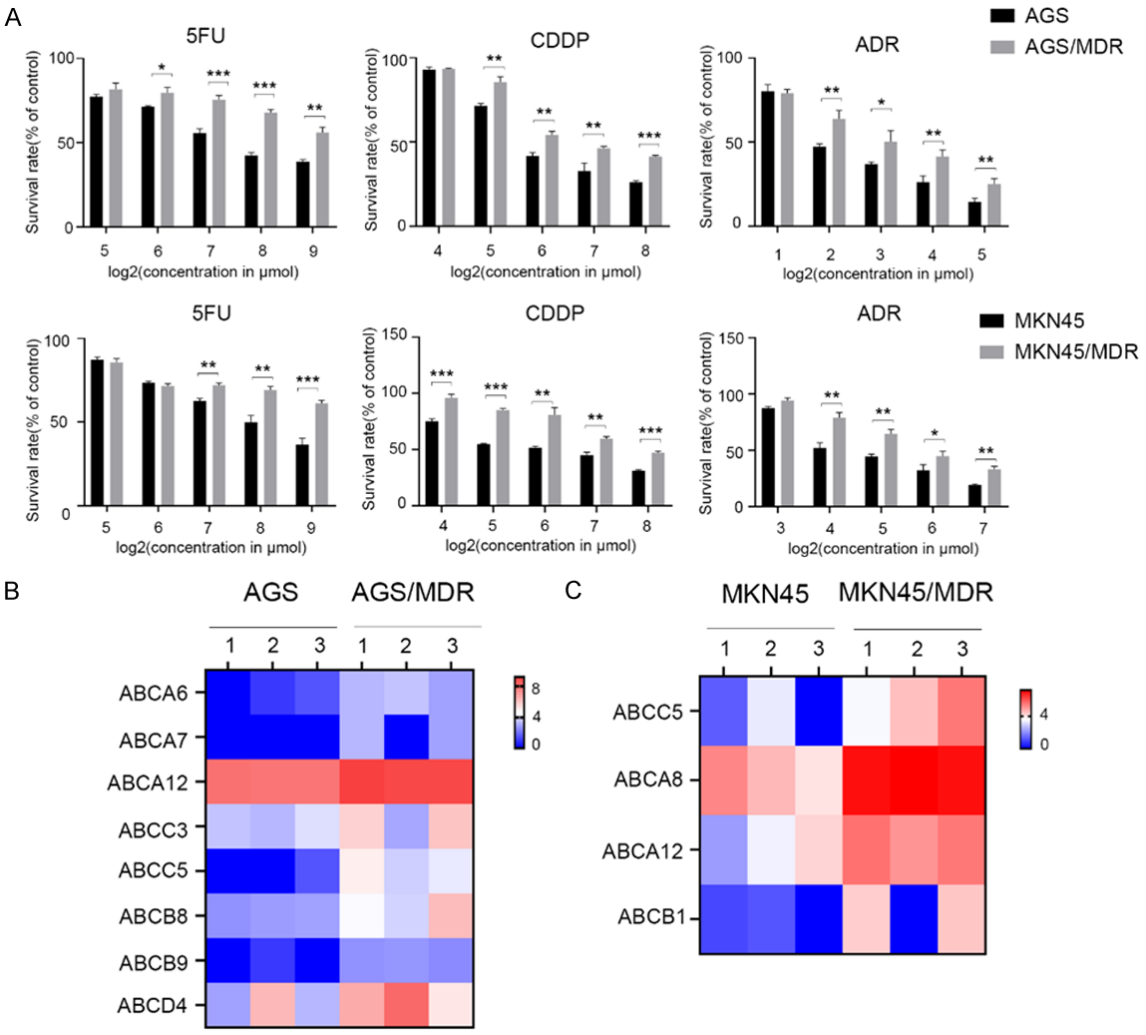

Figure S1. MDR GC cell lines. A. Survival rates of the MDR (AGS/MDR and MKN45/MDR) cell lines compared with those of the parental GC cells (AGS and MKN45) after treatment with various concentrations of CDDP, 5FU, and ADR. B. Heatmap of the ABC gene family transcript expression in the AGS cell line with or without MDR. C. Heatmap of the ABC gene family transcript expression in the MKN45 cell line with or without MDR. All experiments were performed in triplicates. The data are represented as the mean ± SD. *P < 0.05, **P < 0.01, and ***P < 0.001.

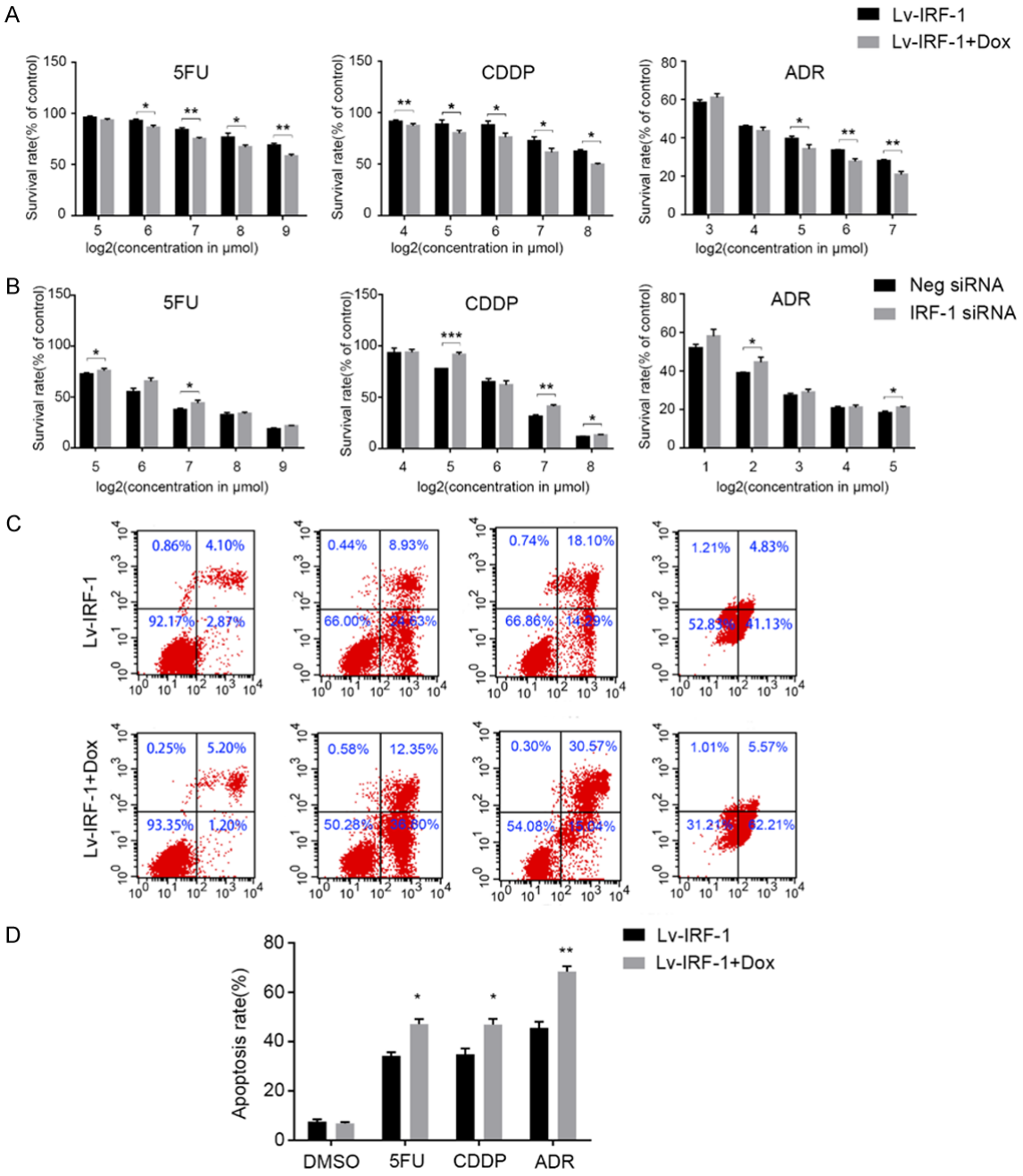

Figure S2. IRF-1 reverses the chemoresistance of gastric cancer *in vitro*. A. Cell viability assay of the cell survival rates of MKN45 MDR/Lv-IRF-1 cells in the presence or absence of 2 μg/ml Dox 24 h after treatment with various concentrations of 5FU, CDDP, and ADR. B. Cell viability assay of the cell survival rates of AGS cells transfected with negative control (Neg) siRNA or IRF-1 siRNA after treatment with various concentrations of 5FU, CDDP, and ADR. C. Flow cytometry detection of apoptotic cells after treatment of MKN45 MDR/Lv-Null and MKN45 MDR/Lv-IRF-1 cells with 2 μg/ml Dox and 800 μmol/l 5 FU and 200 μmol/l CDDP and 30 μmol/l ADR for 24 h. DMSO was used as the control treatment. D. The apoptosis rates of MKN45 MDR/Lv-Null and MKN45 MDR/Lv-IRF-1 cells after treatment with 2 μg/ml Dox and 500 μmol/l 5 FU and 100 μmol/l CDDP and 5 μmol/l ADR for 24 h. All experiments were performed in triplicates. The data are represented as the mean ± SD. *P < 0.05, **P < 0.01, and ***P < 0.001.

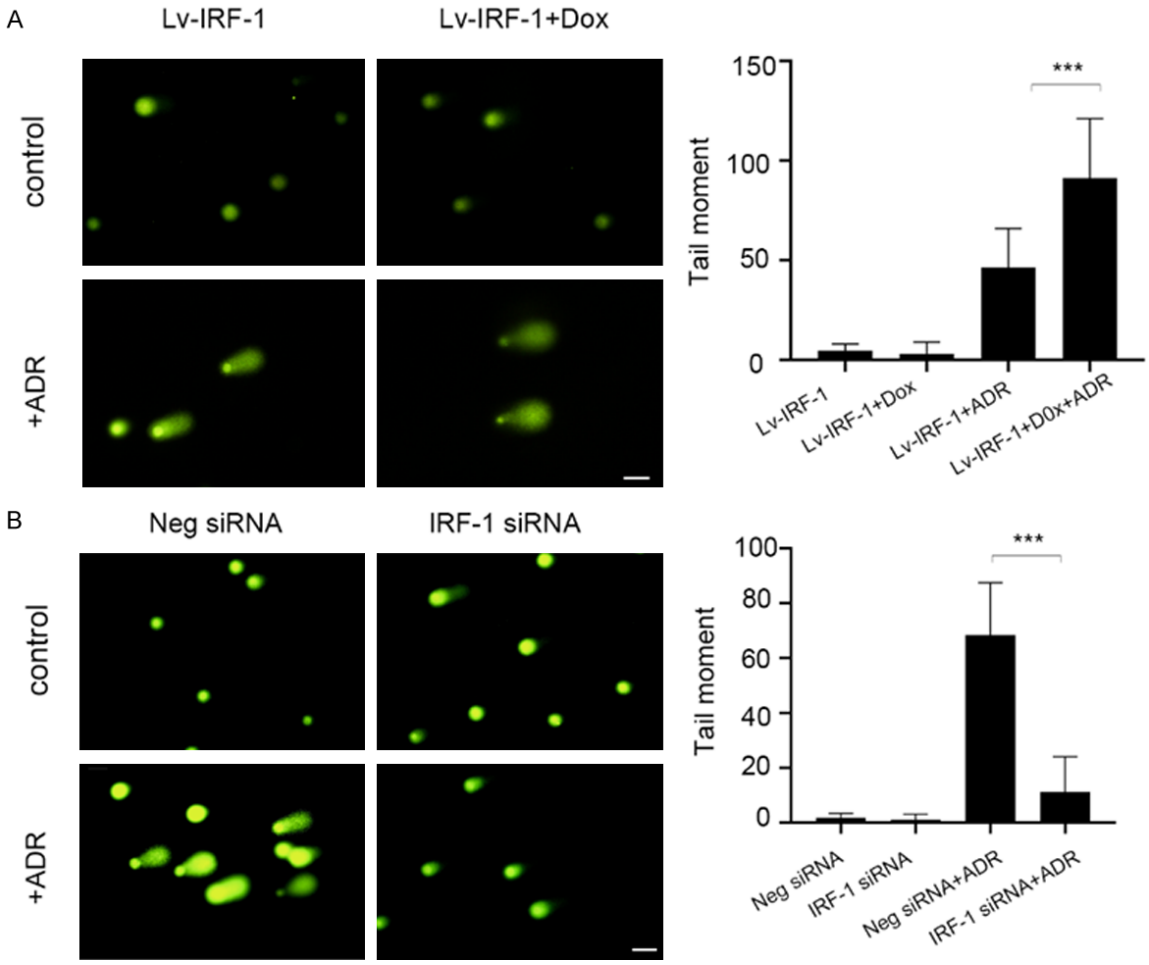

Figure S3. IRF-1 regulates DNA damage repair. A. Representative images of the alkaline comet assay of SGC7901/Lv-Null and SGC7901/Lv-IRF-1 cells after exposure to 5 μmol/l ADR for 18 h. The tail moment is equal to the tail length multiplied by the tail DNA content. Scale bars, 50 μm. B. Representative images of the comet assay after transfecting SGC7901 cells with Neg-siRNA or IRF-1 siRNA and exposing them to 5 μmol/l ADR for 18 h. Scale bars, 50 μm.

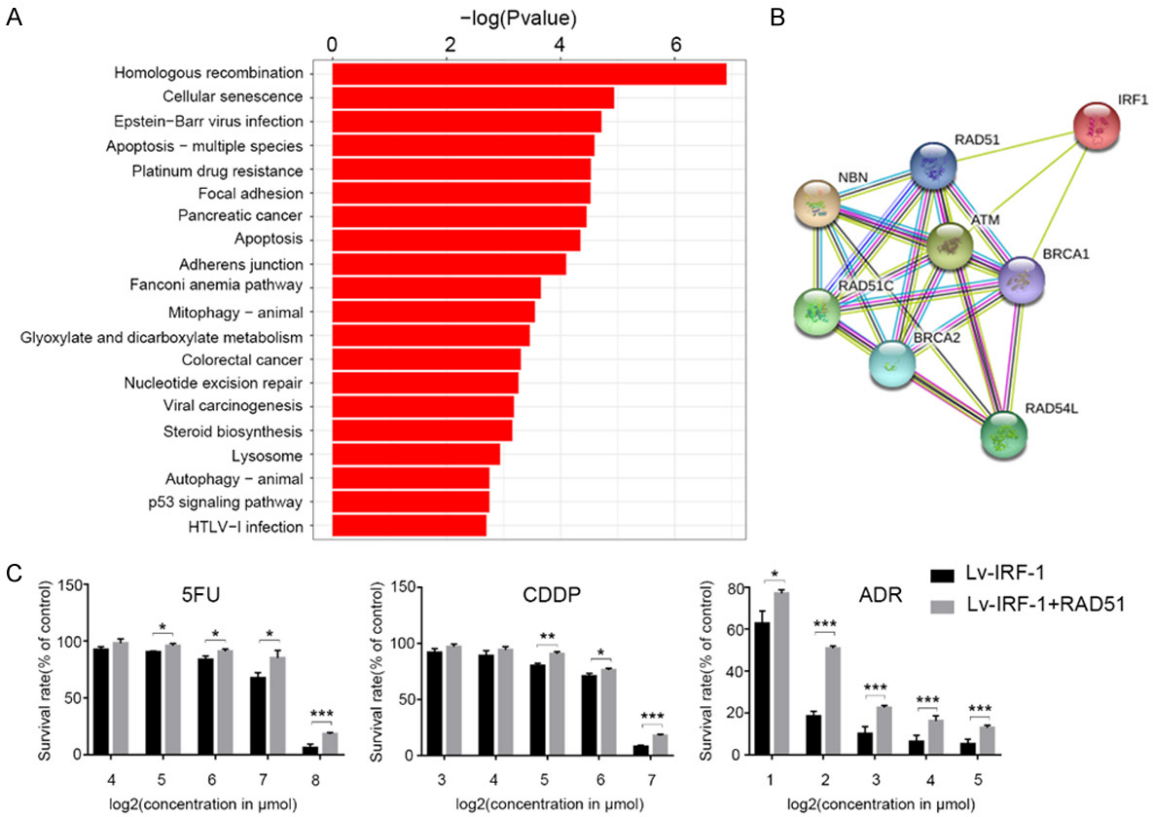

Figure S4. (A) Functional enrichment analysis of the IRF-1 transcripts in cell lines with AGS MDR versus AGS parental gastric cancer cell lines. The ordinate represents the name of the significantly enriched KEGG pathway, and the abscissa represents -Log10 (*P*-value). (B) Target gene protein interaction network diagram. (C) Cell viability assay of the cell survival rates of SGC7901 cells expressing Lv-IRF-1 and Lv-IRF-1 plus RAD51. All experiments were performed in triplicates. In (C), the data are represented as the mean ± SD. *P < 0.05, **P < 0.01, and ***P < 0.001.